153. Haas, R.L., et al., In vivo imaging of radiation-induced apoptosis in follicular lymphoma patients. Int J Radiat Oncol Biol Phys, 2004. **59**(3): p. 782-7.
154. Lahorte, C.M., et al., Apoptosis-detecting radioligands: current state of the art and future perspectives. Eur J Nucl Med Mol Imaging, 2004. **31**(6): p. 887-919.

Chapter 14

IMAGING OF APOPTOTIC CELLS IN VIVO

Juhana Hakumäki
Dept. of Biomedical NMR, A.I.Virtanen Institute for Molecular Sciences, University of Kuopio, P.O.Box 1627, and Dept. of Clinical Radiology, Kuopio University Hospital, P.O.Box 1777, FI-70211 Kuopio, Finland

Abstract: The induction of apoptosis plays a key role in non-surgical cancer treatment – whether this occurs by irradiation, chemotherapy, or hormones. Recent advancements in imaging science and metabolic studies by nuclear magnetic resonance have painted an intriguing picture of the metabolic and biophysical processes involved with the progression of apoptosis *in situ*. It is now possible for us to detect and visualize previously inaccessible and even unrecognized biological phenomena in living cells and tissues undergoing therapeutically induced apoptosis. These new imaging techniques will have an increasing impact in the preclinical design of new anticancer agents and novel treatment protocols to enhance apoptotic cascades and to combat drug resistance. With the advent of molecular medicine and patient-tailored therapeutic options and drug molecules, rapid and accurate visualization of apoptotic response in the clinical settings can be of significant diagnostic and prognostic worth.

Key words: apoptosis, tumor, imaging, NMR, MRI, MRS, PET, SPECT, ultrasound

1. INTRODUCTION

Cell death in tissue takes place along a continuum spanning between necrotic cell death and apoptosis. In contrast to rather uncontrolled necrotic cell death, apoptosis is genetically controlled or "programmed" and cells become committed to a suicide process through numerous cascades of metabolic events. Although at tissue level, apoptosis may generally appear as a subtle process, the individual cells experience profound changes in morphology, structure and biochemistry brought forth by the activation of distinct proteases and lipases. Among the often-quoted hallmark phenomena

M. Sluyser (ed.), Application of Apoptosis to Cancer Treatment, 321-339.

are DNA fragmentation, nuclear condensation, cell shrinkage, and the formation of membrane-encapsulated apoptotic bodies. These concerted actions serve to confine all cellular material towards a recycling process by macrophages and/or neighboring cells, and to protect the surrounding tissue from harmful, uncontrolled release of intracellular messengers, metabolites, and electrolyte fluxes that could elicit inflammation and necrosis[1]. It is exactly this careful orchestration of cell events that provides such an array of markers and targets for visualizing apoptosis by modern imaging technologies (Figure 1).

As demonstrated elsewhere in this book, apoptosis acts as a counterbalance to cell proliferation. It is therefore not only required for normal development and tissue function, but also disturbances in its regulation can promote many disease states[2,3] such as cancer. The primary goal of modern chemotherapy in cancer treatment is tumor cell apoptosis, and due to the inherent cleanliness of the death process as described above, this mode of cell death is sought after by most other anti-cancer treatments, including hormonal agents, toxins, and radiotherapy.

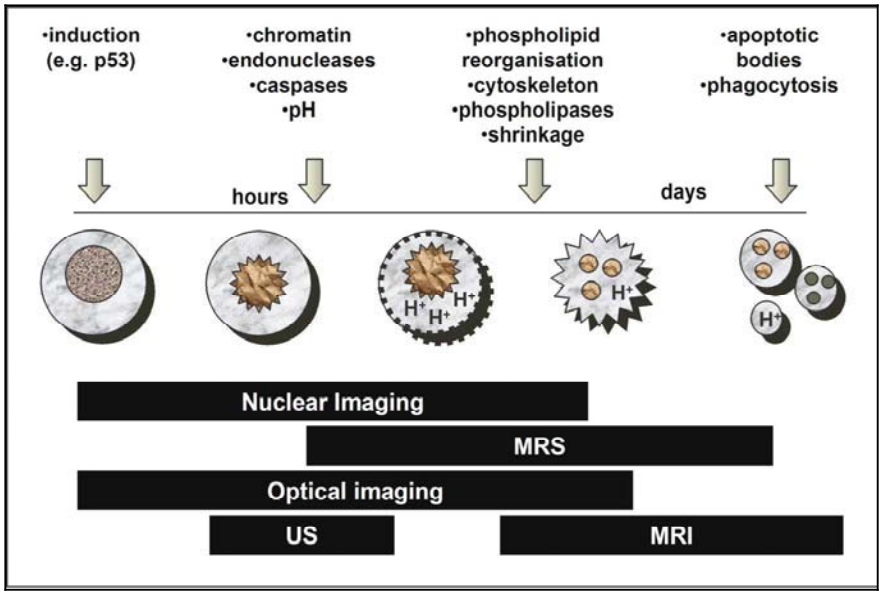

Figure 1. A cartoon and timeline of some key biochemical and biophysical changes occurring in cells that can be exploited for imaging purposes. Generally, molecular events precede those affecting the physical properties of cells, thereby rendering biochemical and molecular imaging markers (such as nuclear imaging and MRS) more sensitive in the early phases than for instance MRI.

Targeted facilitation of apoptosis *in vivo* has been shown to effectively increase the numbers of apoptotic cells in tumors[4-6], and the detected early apoptotic response correlates well with subsequent outcome[6-8]. As described in more detail elsewhere in this book, targeted therapies for modulating apoptosis in malignancies are finding many forms and approaches. Fortunately, non-invasive imaging techniques sensitized to apoptosis are already available, and could become important in future clinical assessment of apoptosis-inducing therapies *in situ*. In the optimal situation, the physician would be able to select the non-responding patients from the responders at much earlier time points than currently possible with anatomical imaging only. Likewise, these techniques could prove immensely useful in basic drug development and testing.

During the last ten years or so, many research groups have studied the possibility of using noninvasive imaging techniques for the purpose of imaging the effects of the apoptotic cascades *in vivo*. The research began with metabolic characterization of cells by nuclear magnetic resonance (NMR) spectroscopy (MRS)[9]. Nuclear imaging techniques together with magnetic resonance imaging (MRI) approaches[9] then followed together with optical imaging[10] and even ultrasound (US)[11,12]. The many papers have now shown beyond doubt that by imaging, phenomena as subtle as apoptosis can non-destructively be visualized by exploiting the myriad of changes involving membrane composition, protein synthesis, glycolysis, phosphatidylcholine, phosphatidylserine and cell fatty acid turnover, energy levels and even intracellular pH throughout the execution of the "apoptotic program" *in vivo*. In addition to the use of exogenous targeted markers for nuclear imaging, and more recently MRI, intrinsic image contrast in MRI and US can also be sensitized to actual biophysical changes in the cellular milieu. All of the mainstream *in vivo* imaging techniques (Table 1) with the exception of cell imaging by microscopy will be outlined here together with some examples of promising applications.

Table 1. A comparison of the imaging modalities for detecting apoptosis *in vivo*.

	penetration	resolution	ionisation	sensitivity	receptors	metabolism
MRI	+++	>0.02 mm	-	+	+	+
MRS	+++	>2 mm	-	+	-	+++[a]
SPECT	+++	>4 mm[b]	+	++	++	++
PET	+++	>5 mm[b]	++	+++	+++	++
Ultrasound	++	>0.2 mm				
Optical	+	>10 mm[c]	-	++	++	++

[a] MRS is the only modality capable of detecting intrinsic metabolites.

[b] SPECT and PET values are typical for dedicated small-animal research microimaging systems. In clinical systems, spatial resolution is several millimeters poorer.

[c] Optical coherence tomography (OCT) can reach resolutions above 10 μm while limited to extreme surfaces (< 2 mm depth).

2. NUCLEAR AND OPTICAL IMAGING

At quick glance, it is apparent that the most numerous applications for *in vivo* imaging of apoptosis are based on marker molecules. This is not surprising given the fact that after all, marker molecules, i.e. biologically active dyes, are what also has made the histological detection of apoptosis possible[13]. Of particular interest here are targeted labels binding to phosphatidylserine, PS.

PS is an abundant phospholipid mostly residing on the cytoplasmic, inner leaflet of the cell membrane[14]. It is however translocated to the outer leaflet of the membrane during apoptosis, when aminophospholipid translocase becomes inactivated and another enzyme, scramblase, is activated to further enhance translocation. Interestingly, this PS externalization occurs very early in the apoptotic chain of events[14], preceding such hallmark events as nuclear condensation and DNA laddering, and perhaps serves as an important signal to neigboring and phagocytizing cells. Of the several proteins known to specifically bind to PS, annexin V is perhaps best known. Optimally up to eight annexin V moieties can bind to one exposed PS, which contributes to its efficiency as a cell label. Applications based on this approach will be discussed below with an introduction to the imaging technologies involved.

2.1 Nuclear imaging

As in X-ray based computed tomography (CT), modern nuclear imaging techniques rely on the rotation of detector arrays around the subject of investigation. With this approach, the position and concentration of a radionuclide marker introduced into the experimental animal or clinical patient can be calculated. Unlike in CT, however, the emission source is an unknown source within the body, and rigorous reconstruction algorithms are required to increase resolution[15].

Nuclear imaging techniques, especially positron emission tomography (PET), have roughly a million-fold sensitivity gain compared to other available imaging techniques. Since receptor proteins are normally present in the nanomolar range, PET has become the method of choice for mapping and studying the function of many receptors, particularly within the central nervous system[16]. However, the use of PET is somewhat limited for imaging apoptosis, since most positron emitting radionuclei are physically short-lived, and many single photon emission tomography (SPECT) radioligands, such as technetium (^{99m}Tc) are easier and less expensive to produce.

SPECT utilizes single photons (at energies of about 140 keV), instead of positron emissions (which result in two 511 keV photons traversing in opposite directions). Because only single photons are emitted from the

radionuclides used for SPECT, collimators are required for source localization. This results in tremendous loss of acquisition efficiency. Also, the useful resolution of SPECT is slightly inferior to PET. However, it is much less expensive to perform SPECT scans, and the typically used SPECT radionuclei have long physical half lives (e.g. 6 h for ^{99}Tc). Together these factors have made this mode of emission tomography an exciting modality for studying apoptosis *in vivo*.

When reviewing literature, it also becomes quite evident that ^{99m}Tc-labeled Annexin V molecules are the most extensively investigated and used *in vivo* marker of apoptosis to date. Since the first *in vivo* imaging demonstration by Blankenberg and co-workers[17] (Figure 2), numerous ^{99m}Tc-Annexin V –based radioligands have been developed and clinical trials have already been undertaken[12]. In part, their popularity is due to the manifold advantages of ^{99m}Tc compared with many other radionuclides, such as low cost, relatively long physical half-life, and easy availability. For further reading on nuclear imaging of apoptosis, the reader is kindly directed to an exceedingly thorough and clearly written overview by Lahorte and co-workers[12]. This paper encompasses most currently existing nuclear labels and labeling methods for Annexin V and derivatives.

Figure 2. Imaging a treated murine lymphoma with radiolabeled annexin V. Mice bearing subcutaneous lef flank murine B-cell lymphomas were treated with 100 mg/kg of cyclophosphamide (i.p.) to induce apoptosis. Twenty hours after treatment mice were injected with 150 μCi of ^{99m}Tc HYNIC annexin V (50 μg/kg of protein), and imaged one hour later. The treated tumor (mass on left flank) demonstrated compound uptake 363% above control levels. L, left; R, right. © The National Academy of Sciences of the USA 1998, reproduced with permission from reference 17.

2.2 Optical imaging

Optical imaging of apoptosis *in vivo* is an emerging field of study[10]. Since visible light such as produced by fluorescein, is not able to penetrate more than 1–2 mm into biological tissue, its use in biological imaging is severely compromised[18]. However, light in the near infrared (NIR) range (wavelengths 700-1200 nm) allows better penetration in tissue[19], but at the cost of considerable absorption and scattering. Optical tomograpy can however be used to reconstruct the probed structure and location by back-projecting the transmitted light through the object along multiple paths similarly to CT. Despite its shortcomings in terms of penetration and resolution, optical imaging offers the opportunity for real-time monitoring of biological phenomena such as apoptosis. The First *in vivo* data in irradiated tumor-bearing nude mice showed increased Cy5.5-Annexin V uptake in tumors over a period of ten days due to excellent fluorochrome stability[19]. It is worth noting, that this is also a considerable temporal advantage in comparison to almost all radionuclides.

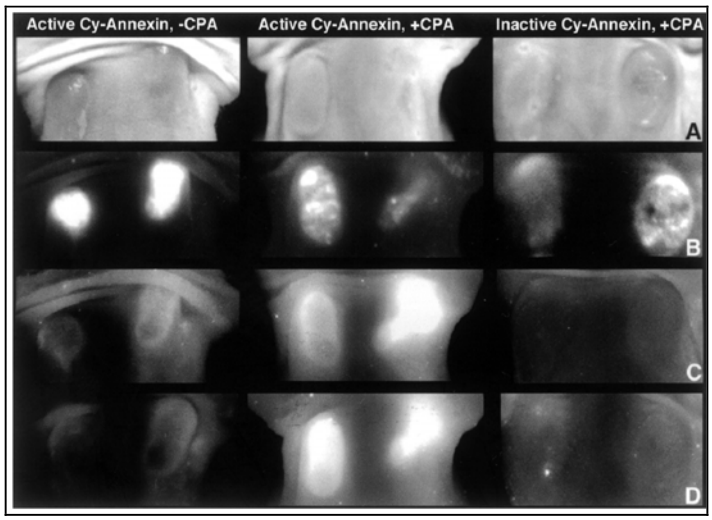

Figure 3. Imaging of apoptosis in CR-red fluorescent tumor model implanted in mammary pad. Animals were divided into three groups: (a) injected with active Cy-annexin and not treated with CPA; (b) injected with active Cy-annexin and treated with CPA; and (c) injected with inactive Cy-annexin and treated with CPA. A, visible light image of implanted tumors; B, expression of DsRed2 in CR tumor (red fluorescence channel); C, near-infrared signal measured in tumors at 75 min after the injection of Cy-annexin; D, near-infrared signal measured in tumors at 20 h after the injection of Cy-annexin. Animals received an i.p. injection of 170 mg/kg CPA. © American Association for Cancer Research 2003, reproduced with permission from reference 20.

Similar results (Figure 3) have been obtained by Petrovsky et al. by using Cy 5.5-annexin as a NIR fluorescence probe for apoptosis in different tumor types and therapies and imaged from outside an intact living animal[20].

Another optical imaging approach that deserves mention is bioluminescence imaging (BLI), which is based on the use of the luciferase enzyme. This technique has recently been used to investigate the spatial relationship between chemotherapy-induced tumour apoptosis and total tumour burden over time, as assessed by BLI together with microSPECT[21].

3. ULTRASOUND

Studies have surprisingly shown that ultrasound (US) imaging may also be able to detect apoptosis via the biophysical effects exerted by subcellular nuclear changes such as chromatin condensation and DNA fragmentation *in vitro*. Using apoptotic and control AML-3 leukemia cells, Czarnota and co-workers discovered that twenty-four hours from the onset of cisplatin-induced apoptosis (95% apoptotic cells), a 2 to 5-fold increase in US backscatter signal could be detected[22]. Interestingly, this increase appeared to correlate nicely with the actual progression of nuclear condensation[23]. In the latter study, the authors used high frequency US imaging to demonstrate epidermal apoptosis also *in vivo*. It remains to be seen however, whether US will become a truly useful tool for detecting changes in often deep-seated tumors *in vivo*, where also much lower percentages of apoptotic cells are manifest (typically < 10% at any time point) despite anticancer therapy.

4. NUCLEAR MAGNETIC RESONANCE

Certain atomic nuclei, such as the proton (^{1}H), possess what is called non-zero angular momentum, i.e. nuclear spin. This creates a magnetic dipole moment along the axis of rotation. When such nuclei are placed in an external magnetic field, net magnetization is created by the equilibrium difference between magnetic dipole moments existing in two different energy states. This net magnetization, which forms the basis of all nuclear magnetic resonance (NMR) experiments, is proportional to the strength of the external magnetic field, and can be perturbed by radio frequency (RF) radiation. When perturbed magnetization and its recovery (i.e. relaxation) to unperturbed equilibrium state is detected through receivers, information on the nuclear spin environment of the sample or tissue can be obtained. When this signal is used to detect and quantify the presence of chemically distinct compounds, it is called NMR spectroscopy (or clinically, MRS). When this

information is used to create spatially resolved maps of quantities and/or relaxation properties of the observed nucleus, the procedure is called magnetic resonance imaging (MRI) and when the above techniques are combined, magnetic resonance spectroscopic imaging (MRSI). Because signal manipulation and detection in NMR occur in the radio frequency range of the electromagnetic spectrum, no ionizing radiation is involved. This makes NMR particularly attractive for noninvasive *in vivo* studies of living systems.

^{1}H is the most sensitive non-radioactive NMR nucleus with a 99.9% natural abundance. It is particularly well suited for NMR studies, because virtually all biological material and compounds possess hydrogen. MRI benefits greatly from the highly concentrated water protons (~80 mol/l in tissue). Typical ^{1}H spectra can be seen in Figures 4A and Figure 5. Other naturally occurring nuclei can however be used for NMR spectroscopy: the most important are phosphorus (^{31}P) with 100% natural abundance, and a stable isotope of carbon (^{13}C) with 1,1% natural abundance. Although both of these nuclei are much less sensitive than proton, the particular power of ^{31}P NMR spectroscopy lies in detecting cell pH and energy metabolites, such as shown in Figure 4B. To enhance sensitivity, and especially to decipher metabolic pathways, ^{13}C labeling of substrates is often used.

NMR is sadly not a very sensitive technique. However, this is at least partly compensated by the fact that in metabolic studies dynamic changes over the whole range of metabolites can be observed and accurately quantified, as long as they exist above a practical detection threshold (millimolar range *in vivo*, and one tenth of that *in vitro*). For a more detailed account on the basics of biological NMR and MRI, the reader is kindly directed to David Gadian's excellent textbook[24].

4.1 Magnetic Resonance Spectroscopy (MRS)

Magnetic resonance research into apoptosis started in the mid-nineties when several groups began looking at relevant metabolic indicators of apoptosis. Adebodun and Post were the first to identify, by using ^{31}P MRS, an aberrant metabolic profile in leukemia cells treated with dexamethasone to undergo apoptosis *in vitro*[25]. The researchers reported a clear reduction in phosphomonoesters (i.e. phosphoethanolamine and phosphocholine) and ATP. Following up on the study, Nunn and co-workers used ^{1}H MRS to study metabolic changes in neutrophils undergoing apoptosis[26], and instead observed an increase in phosphocholine concentration, which the authors attributed to their model of Fas-receptor mediated apoptosis and phospholipase-C activation. Two years later, Williams et al.[27] set out to better characterize metabolic changes in Chinese hamster ovary cells (CHO-

K1) and HL-60 leukemia cells using ^{31}P MRS, which were treated with several apoptosis-inducing drugs with functionally very different modes of action, namely farnesol, chelerythrine, etoposide, campothecin, and ceramide. Only two metabolites were observed to consistently increase during apoptosis: fructose-1,6-bisphosphate (FBP, a glycolytic pathway intermediate) and cytidylyldiphosphocholine (CDP-choline, an intermediate step metabolite in phosphatidylcholine biosynthesis). In this case, the increase in FBP concentration in HL-60 cells was be explained by either depletion of cellular NAD(H), or by the activation of 6-phosphofructo-1-kinase through AMP accumulation, an observation corroborated soon by the work of Ronen and co-workers[28]. The NMR-observed accumulation of CDP-choline in apoptotic cells (Figure 4B) was later linked by the same group to the inhibition of choline phosphotransferase (CPT) by isotope labeling studies[29]. CPT is likely to become inhibited in apoptotic cells, since it has an alkaline pH optimum (8 - 8.5), yet cellular acidosis (pH <6.5) appears to be a frequent event in apoptosis[27].

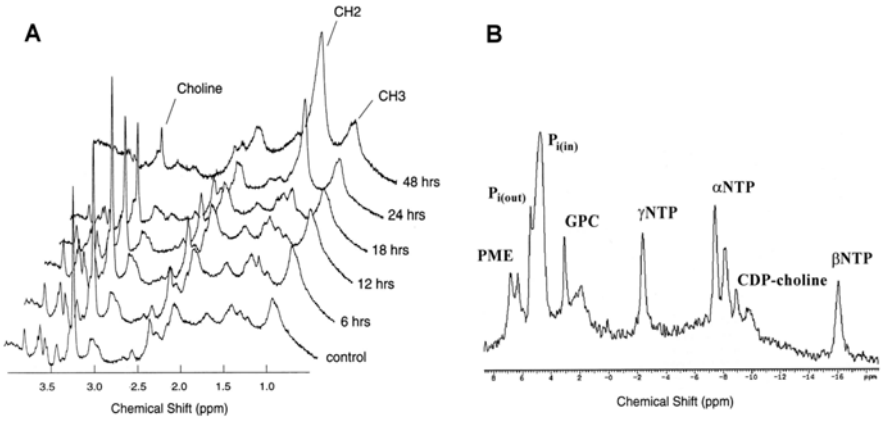

Figure 4. A) Time course of ^{1}H NMR spectroscopy resonances in Jurkat leukemia cells. Note the resulting increase in lipid methylene (-CH_2) resonances over time and with increasing percentage of apoptotic cells (not shown). © American Society of Hematology 1997, reproduced with permission from reference 28. B) ^{31}P NMR spectrum of apoptotic Chinese hamster ovary CHO-K1 cells is shown (CDP-choline, cytidylyldiphosphocholine; GPC, glycerophosphocholine; NTP, nucleotide triphosphate, P_i, inorganic phosphate; PME, phosphomonoesters. © Wiley & Sons 1998, reproduced with permission from reference 27.

Blankenberg et al. were the first to use ^{1}H MRS of living cells *in vitro* to detect metabolic changes caused by apoptosis. In their seminal paper, large signals from mobile intracellular lipids were shown to accumulate over time

(Figure 4A) and a correlation between the intensity ratio of the 1.3 ppm (-CH_2-) to 0.9 ppm (-CH_3) -resonances and the fraction of apoptotic cells following induction of apoptosis was established[30]. At the time, it was thought that the signals originated from plasma membrane microdomains[31], and that these were perhaps connected to modified membrane microfluidity brought forth by apoptosis. However, the more recent studies have given enough grounds to discard this hypothesis: it is currently quite accepted that these resonances originate from a storage form of cell lipids within the cell, i.e. from triglycerides within cytoplasmic lipid droplets[32].

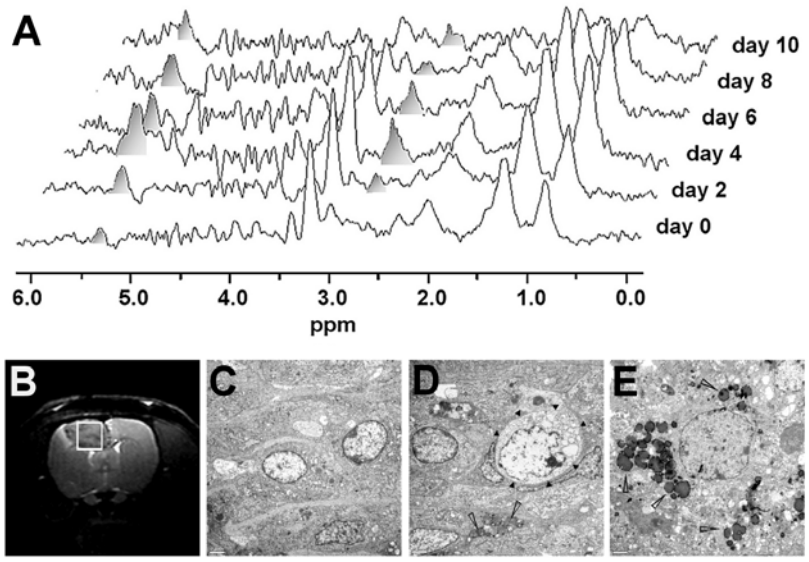

Figure 5. A typical time course of ^{1}H MRS data from an HSV-tk transfected glioma treated with ganciclovir *in vivo* for a period of 10 days (A). Signals from polyunsaturated lipid proton moieties are shown shaded (at 5.3 and 2.8 ppm). An untreated glioma is shown on conventional MRI, with a white box to denote the localization from which spectroscopy signals were obtained (B). Transmission electron microscopy (magnification x 5000) shows untreated tumor cells (C), lipid droplets (open arrows) and apoptotic bodies (black triangles) (D), and densely osmiophilic, polyunsaturated fatty acid-rich droplets (E) in treated tumours after four days of treatment. © 1999 Nature publishing, reproduced with permission from reference 33.

Hakumäki et al. extended the previous approach by showing that ^{1}H MRS could be used to noninvasively detect apoptosis *in vivo*[33]. In this study, herpes-simplex virus thymidine kinase (HSV-tk)- transfected BT4C gliomas were treated by systemic administration of ganciclovir to induce widespread apoptosis in tumor tissue. As a result, significant increases in

polyunsaturated lipid signals could be observed following tumor treatment (Figure 5, previous page). The lipid signals also correlated with the number of apoptotic cells, concentration of cholesteryl esters and triglycerides, and the number of osmiophilic cytoplasmic lipid droplets in tumor cells.

Surpisingly, it is not yet quite clear why lipids accumulate in apoptotic cells[32]. There is however increasing evidence to support a role for phospholipase-A2 activity[33,34]. Recently, two groups have shown using Jurkat T-cells *in vitro*, that apoptosis is indeed accompanied by an quantitative relationship between cytoplasmic lipid droplets and lipid signal in ^{1}H MRS[35,36], with more independent biochemical evidence suggesting a role for intracellular phospholipase-A2 activation after induction of apoptosis[37]. In fact, more recent work by Liimatainen et al. demonstrates a plausible stoichiometric relationship between membrane fatty acid release by phospholipase-A2 as determined by gas liquid chromatography and quantitative ^{1}H MRS[38].

Due to the poor relative sensitivity and spatial resolution of MRS, it is an absolute necessity to use markers with sufficient signal intensity. If this requirement is fulfilled, molecular markers can easily be mapped with techniques such as MRSI (Figure 6). So far, the ^{1}H MRS signals from cytoplasmic lipids appear the most robust NMR candidates for *in vivo* detection of apoptosis. However, they are not perfect since the metabolic factors governing their dynamics are poorly understood and theoretically, ^{1}H such signals could also arise from other cellular processes, such as necrosis, and from other endogenous cell types[32]. It has also been documented that the spectral lipid baseline features may differ, especially with multidrug resistant cell lines[39]. However, many available *in vitro* assays for apoptosis can also be ambiguous. For instance, even DNA fragmentation, often considered the gold standard for apoptosis detection, cannot always be observed in cells undergoing apoptosis[40]. ^{31}P markers such as CDP-choline and FBP could also act as apoptosis markers. However, ^{31}P MRS is hampered by its poor sensitivity and spatial resolution. Also, it might be difficult to distinguish resonances such as FBP from the partly overlapping phosphomonoester signals (Figure 4B).

Scott and Adebodun have elegantly used ^{13}C MRS *in vitro* to assess protein synthesis during dexamethasone-induce apoptosis in CEM-C7-14 human leukemia cells[41]. By measuring the incorporation of ^{13}C-labeled amino acids into cell proteins, they could observe not cessation, but a reduction of protein synthesis by as much as 87%. Unfortunately ^{13}C NMR is too insensitive to design any practical imaging applications.

Interestingly, ^{1}H MRS can also be sensitized to molecular diffusion, in similar fashion as diffusion-weighted magnetic resonance imaging, or DWI[42]. This technology assesses the Brownian molecular motion *in vivo* and

with the use of intracellular probes such as naturally occurring tumor metabolites, can be used to study the biophysical status of tissue. Hakumäki and co-workers showed that during apoptosis-inducing therapy, there is a striking ~50% reduction in the apparent diffusion coefficient (ADC) of intracellular choline *in vivo*, accompanied by a significant increase in the rapidly diffusing water component reflecting extracellular water[43].

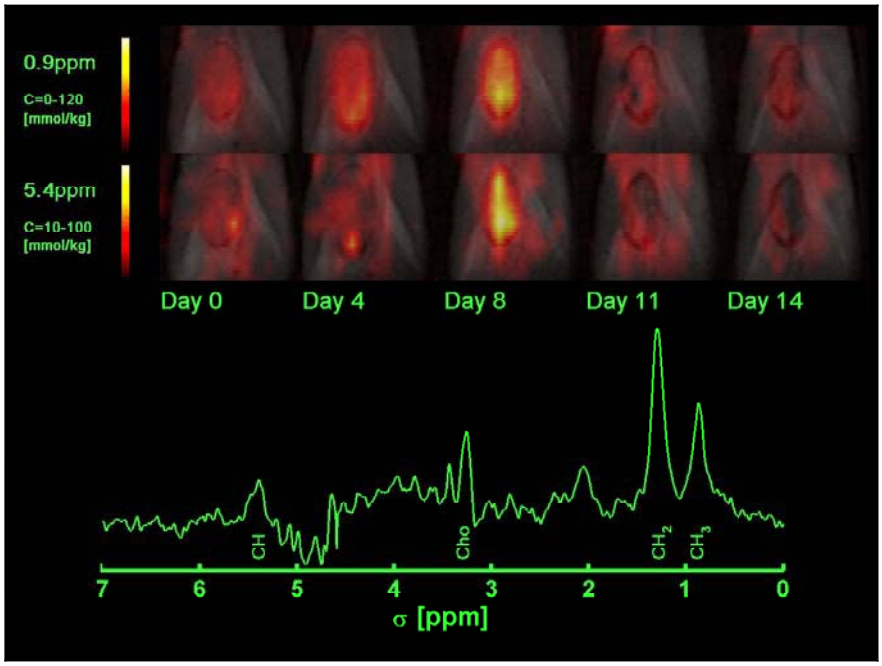

Figure 6. Magnetic resonance spectroscopic imaging (MRSI) of lipid accumulation in an apoptotic experimental rat glioma over 14 days time. In this hybrid technique, spectroscopic resonances unique to different chemical species (as exemplified by the spectrum below) can be mapped to produce magnetic resonance images such as for the lipid acyl chain terminal methyl (-CH_3, 0.9ppm) and unsaturated carbon vinyl (=CH-, 5.4 ppm) protons. Although the spatial resolution is considerably lower than in conventional MRI, advanced techniques actually allow volume resolutions similar to micro-PET (4.7 µl, such as here) without the use of any exogenous agents or marker molecules. The lipid concentrations are coded by the color bars on left, superimposed onto a anatomical MRI images. Figure courtesy of Mr. Timo Liimatainen, Dept. of Biomedical NMR, University of Kuopio, Finland.

These results directly imply decrease in cell size and number, together with increased intracellular viscosity as experienced by the intracellular choline metabolites. Recently, Hortelano et al. have shown similar MRS results in cells[44], supporting the idea that cells apoptotic shrinkage and loss

of cells can be held accountable for the observed molecular diffusion phenomena.

4.2 Magnetic Resonance Imaging (MRI)

The information provided by MRI has long been mostly anatomical, and the technology clearly excels at this. MRI has in fact, become an indispensable imaging modality that can probe tissue and its biophysical properties with exceptional in-plane resolution *in vivo*. One of the key advantages is that this can be done noninvasively, without physically altering tissue and without the use of radioactive markers[24]. This is important clinically, where MRI is more widely available, accurate localization is required, and the levels of therapeutically induced apoptosis may still be low. Hakumäki et al. have recently shown in a BT4C rat glioma model, that in (HSV-tk)- transfected tumors, T1- and T2- relaxation times and water diffusion increase during ganciclovir therapy. However, T1- relaxation times in the rotating frame ($T1_{rho}$) are elevated even when tumor volumes still increase, but significant apoptosis is starting to take place[45]. Recently, Gröhn and co-workers used short interpulse intervals for adiabatic Carr-Purcell (CP) –pulse trains to produce a novel contrast mode which was sensitive to early therapeutic response, similarly to $T1_{rho}$[46].

Unfortunately, the biophysical phenomena governing intrinsic image contrast generation are rather poorly understood, and are likely to involve a number of processes related to tissue microarchitecture, protein/lipid content and composition, pH, flow, oxygenation and any combination of these. At best, this still leaves room for ambiguity reflecting differences in cancer tissue type and the chosen therapeutic approach. Also, one might argue that changes in MR image contrast or water diffusion due to cell shrinkage and membrane blebs are unlikely to observe any of the early phases in the apoptotic process. This has in fact been shown by Valonen and co-workers, who recently showed that the DWI increase in apoptotic BT4C gliomas directly correlates with cell loss[47]. T1 and T2 appear to behave similarly. However, $T1_{rho}$ and short interpulse interval-CP contrast appear to be a curious exceptions to this, and currently lack proper explanation[45,46].

In light of the above, it would be extremely beneficial to combine chemical specificity (such as that obtained by nuclear imaging or MRS) with the much better resolution (>50 μm) of MRI. Here in fact, a deep conceptual revolution has occurred in the recent years. MRI contrast has been shown to be adjustable by chemically malleable marker ligands linked to magnetically active compounds, such as superparamagnetic iron oxide nanoparticles, i.e. SPIO[48,49] or gadolinium (Gd) chelates that have been used to detect the overexpression of certain receptors in tumors *in vivo* [49,50]. Along this line of

approach, Zhao and co-workers demonstrated success by labeling the C2-domain of a phosphatidylserine binding protein, synaptotagmin I, with an SPIO particle[51]. The SPIO-labeled protein was shown to bind to apoptotic cells *in vitro*, and when administered intravenously into mice bearing EL4 lymphomas, decreases in MR image intensities in tumor regions containing large numbers of apoptotic cells could be observed (Figure 7). In analogous fashion to Blankenberg et al.[17] and above, Schellenberger and co-workers have cross-linked SPIO nanoparticles with Annexin V, and demonstrated dose-dependent signal intensity reduction in T2-weighted images of camptothecin-treated apoptotic (65%) Jurkat cells versus untreated controls *in vitro*[52].

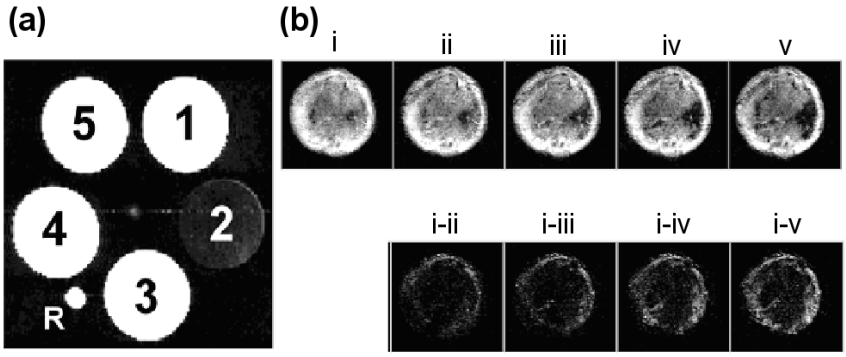

Figure 7. MR images of CHO-K1 cells in test tubes (a). The cells were treated with etoposide to induce apoptosis, incubated with C2-SPIO or plain SPIO (200 μM Fe), washed and then immobilized in 5 mm diameter NMR tubes and imaged. Apoptotic cells incubated with BSA conjugated SPIO (1), apoptotic cells incubated with C2-SPIO (2), control cells incubated with C2-SPIO (3), apoptotic cells with no label (4), control cells incubated with BSA-SPIO (5), reference capillary with water (R). The signal loss due to retention of targeted contrast agent is clearly visible in sample number 2. In (b), MR images of a tumor in a drug-treated mouse following injection of C2–SPIO (20 mg Fe/kg tissue), are shown. MR images i-v are from before and after injection of C2–SPIO. The first control (i) was acquired before injection of contrast agent and afterwards at time points of 11 (ii), 47 (iii), 77 (iv), and 107 (v) minutes postinjection. Contrast agent uptake (and apoptotic cells) become visible as areas of image intensity loss, further highlighted in the respective subtraction images (i-ii, i-iii, i-iv, i-v), as bright areas.

5. FUTURE DIRECTIONS

Although in may seem that the recent developments in imaging of apoptosis *in vivo* are indeed breathtaking, we are essentially very much at the beginning. Clinical imaging applications for cancer need to be tested and developed effectively. This requires much more experimental research with solid, consistent models, and relevant oncological problems. Flow cytometry, immunohistological stains, and the gold standard i.e. TUNEL assay need to be kept abreast to critically assess the localization, extent and kinetics of therapeutically induced apoptosis, and to confirm the imaging findings. Naturally, the optimal time frames for imaging therapeutically induced apoptosis will have to be addressed as well.

It is evident that many more markers for apoptosis, with better sensitivity and specificity must be explored. In this sense, highly specific, targeted apoptosis-detecting ligands would be preferable. Perhaps one should realize that there is a caveat even to the widely used Annexin-V approach: in some cases, necrotic cells undergoing lysis may also bind Annexin-V when the phosphatidylserine still residing on the inner membrane leaflets becomes exposed[53]. This could lead to overestimation or incorrect assignment of apoptosis in necrotic insults.

Among the most exciting novel targets are probably those directed at the very initial steps of the apoptotic program, such as DNA-damage reporting p53 expression[54] and at the apoptotic cascades themselves via radiolabeled caspase inhibitors[12]. Since caspase activation is known to occur early in the apoptotic program, such radiolabeled inhibitors would offer a highly specific tool detecting early events in apoptosis. It is also believed that these marker molecules might be more specific to apoptosis for reasons mentioned above. Overall in terms of sensitivity, nuclear imaging probes will fare far better than the other modalities.

Due to certain advantages such as the extremely high spatial resolution and true non-invasiveness, a small niche will remain for MRI agents however. Optimal MRI contrast generation and agent delivery will be the subject of future research. For instance, the above-described SPIO-labeling, although being sensitive, provides “negative” contrast i.e. signal intensity reduction (Figure 7). This is unfortunately more prone to artifacts and also more difficult to interpret due to the often seen intrinsic heterogeneity of tumor masses on MRI. The conjugation of marker proteins with paramagnetic gadolinium-based agents, might become a means to avert this problem by providing “positive” contrast, i.e. brightening on MRI, although this approach is likely to be plagued by severe sensitivity problems.

The biodistribution and metabolism of NMR spectroscopic markers can be efficiently probed and more information gained by using advanced MRSI

techniques. Among the potential applications, lipid ^{1}H MRSI is the most robust and practical (Figure 6). The use of ^{31}P clinically appears to be unlikely due to its poor sensitivity, long acquisition times, and inferior spatial resolution. It is noteworthy however, that intracellular pH can be observed noninvasively only by ^{31}P MRS. Intracellular pH on the other hand appears to be one of the critical factors at work in the apoptotic program, affecting even caspase activation during apoptosis.

Regardless of the technique employed, the generation of protein-based targeted imaging agents is expensive, and all compounds heading for clinical applications will need to be assessed for patient biodistribution and safety. While waiting for new developments at this front, we are likely to witness some of the other techniques, such as SPECT, MRS and diffusion-weighted MRI gain foothold within the clinic. However, for those involved with experimental studies and drug design, *in vivo* imaging of apoptosis has already become reality, with an ever-increasing and powerful array of technologies to choose from.

ACKNOWLEDGEMENTS

The author would like to thank the Finnish Academy, the Finnish Cancer Institute and Instrumentarium Science Foundation for support.

REFERENCES

1. J. Savill and V. Fadok, Corpse clearance defines the meaning of cell death, *Nature* **407**, 784-788 (2000).
2. R.A. Kinloch et al, The pharmacology of apoptosis, *Trends Pharmacol. Sci.* **20**, 35-42 (1999).
3. G.I. Evan and K.H. Vousden, Proliferation, cell cycle and apoptosis in cancer, *Nature* **411**, 342-348 (2001).
4. B. Dubray et al., In vitro radiation-induced apoptosis and early response to low-dose radiotherapy in non-Hodgkin's lymphomas, *Radiother. Oncol.* **46**, 185-191 (1998).
5. B. Jansen et al., Chemosensitisation of malignant melanoma by BCL2 antisense therapy, *Lancet* **356**, 1728-1733 (2000).
6. W.F. Symmans et al., Paclitaxel-induced apoptosis and mitotic arrest assessed by serial fine-needle aspiration: implications for early prediction of breast cancer response to neoadjuvant treatment, *Clin. Cancer Res.* **6**, 4610-4617 (2000).
7. R.E. Meyn et al., Apoptosis in murine tumors treated with chemotherapy agents, *Anti-Cancer Drugs* **6**, 443-450 (1995).
8. P.A. Ellis et al., Preoperative chemotherapy induces apoptosis in early breast cancer, *Lancet* **349**, 849 (1997).
9. J.M. Hakumäki J.M. and K.M. Brindle, Techniques: visualizing apoptosis by nuclear magnetic resonance, *Trends Pharmacol. Sci.* **24**, 146-149 (2003).

10. C. Bremer et al., Optical-based molecular imaging: contrast agents and potential medical applications, *Eur Radiol.* **13**, 231-243 (2003).
11. F.G. Blankenberg, K. Ohtsuki, H.W. Strauss, Dying a thousand deaths. Radionuclide imaging of apoptosis, *Q. J. Nucl. Med.* **43**, 170-176 (1999).
12. C.M. Lahorte et al., Apoptosis-detecting radioligands: current state of the art and future perspectives, *Eur. J. Nucl. Med. Mol. Imaging* **31**, 887-919 (2004).
13. C. Stadelmann and H. Lassmann, Detection of apoptosis in tissue sections, *Cell Tissue Res.* **301**, 19-31 (2000).
14. S.J. Martin et al., Early redistribution of plasma-membrane phosphatidylserine is a general feature of apoptosis regardless of the initiating stimulus - Inhibition by overexpression of Bcl-2 and Abl, *J. Exp. Med.* **182**, 1545-1556 (1995).
15. J.T. Kuikka et al., Future developments in nuclear medicine instrumentation: a review., *Nucl. Med. Commun.* **19**, 3-12 (1998).
16. A.F.Chatziioannou, Molecular imaging of small animals with dedicated PET tomographs, *Eur. J. Nucl. Med. Mol. Imaging* **29**, 98-114 (2002).
17. Blankenberg, F. G. et al., In vivo detection and imaging of phosphatidylserine expression during programmed cell death, *Proc. Natl. Acad. Sci. USA* **95**, 6349-6354 (1998).
18. T.J. Sweeney et al., Visualizing the kinetics of tumor-cell clearance in living animals, *Proc.Natl. Acad. Sci. USA* **96**, 12044-12049 (1999).
19. J.S. Reynolds et al., Imaging of spontaneous canine mammary tumors using fluorescent contrast agents, *Photochem Photobiol.* **70**, 87-94 (1999).
20. A. Petrovsky et al., Near-infrared fluorescent imaging of tumor apoptosis, *Cancer Res.* **63**, 1936-42 (2003).
21. S.J. Mandl et al., Multi-modality imaging identifies key times for annexin V imaging as an early predictor of therapeutic outcome, *Mol Imaging* **3**, 1-8 (2004).
22. G.J. Czarnota et al., Ultrasonic biomicroscopy of viable, dead and apoptotic cells, *Ultrasound Med. Biol.* **23**, 961-965 (1997).
23. G.J. Czarnota et al., Ultrasound imaging of apoptosis: high-resolution non-invasive monitoring of programmed cell death in vitro, in situ and in vivo, *Br. J. Cancer* **81**, 520-527 (1999).
24. D.G. Gadian, *NMR and its applications to living systems* (Oxford Science, Oxford, 1995).
25. F. Adebodun and J.F.M. Post, ^{31}P NMR characterization of cellular metabolism during dexamethasone-induced apoptosis in human leukemic cell lines, *J. Cell. Physiol.* **158**, 180-186 (1994).
26. A.V.W. Nunn et al., Characterisation of secondary metabolites associated with neutrophil apoptosis, *FEBS Lett.* **392**, 295-298 (1996).
27. S.N.O. Williams et al., Induction of apoptosis in two mammalian cell lines results in increased levels of fructose-1,6-bisphosphate and CDP-choline as determined by ^{31}P MRS, *Magn. Reson. Med.* **40**, 411-420 (1998).
28. S. Ronen et al., Magnetic resonance detects metabolic changes associated with chemotherapy-induced apoptosis, *Br. J. Cancer* **80**, 1035-1041 (1999).
29. M.L. Anthony et al., Inhibition of phosphatidylcholine biosynthesis following induction of apoptosis in HL-60 cells, *J. Biol. Chem.* **274**, 19686-19692 (1999).
30. F.G. Blankenberg et al., Quantitative analysis of apoptotic cell death using proton nuclear magnetic resonance spectroscopy, *Blood* **89**, 3778-3785 (1997).
31. C.E. Mountford CE and L.C. Wright, Organization of lipids in the plasma membranes of malignant and stimulated cells: a new model, *Trends Biochem Sci.* **13**, 172-7 (1988).

32. J.M. Hakumäki and R.A. Kauppinen, ^{1}H NMR visible lipids in the life and death of cells, *Trends Biochem. Sci.* **25**, 357-362 (2000).
33. J.M. Hakumäki et al., ^{1}H MRS detects polyunsaturated fatty acid accumulation during gene therapy of glioma: implications for the in vivo detection of apoptosis, *Nature Med.* **5**, 1323-1327 (1999).
34. J.L. Griffin et al., Assignment of ^{1}H nuclear magnetic resonance visible polyunsaturated fatty acids in BT4C gliomas undergoing ganciclovir-thymidine kinase gene therapy-induced programmed cell death, *Cancer Res.* **63**, 3195-3201 (2003).
35. M. Di Vito et al., ^{1}H NMR-visible mobile lipid domains correlate with cytoplasmic lipid bodies in apoptotic T-lymphoblastoid cells, *Biochim. Biophys. Acta*. **1530**, 47-66 (2001).
36. N.M. Al-Saffar et al, Apoptosis is associated with triacylglycerol accumulation in Jurkat T-cells, *Br. J. Cancer* **86**, 963-970 (2002).
37. D. De Valck et al., Differential activation of phospholipases during necrosis or apoptosis: a comparative study using tumor necrosis factor and anti-Fas antibodies, *J. Cell Biochem.* **71**, 392-399 (1998).
38. T. Liimatainen et al., ^{1}H magnetic resonance spectroscopic imaging of phospholipase activity in rat gliomas in vivo, *Proc. 12th Ann. Sci. Meeting ISMRM, Kyoto, Japan* (2004).
39. L. Le Moyec et al., Proton nuclear magnetic resonance spectroscopy reveals cellular lipids involved in resistance to adriamycin and taxol by the K562 leukemia cell line, *Cancer Res.* **56**, 3461-3467 (1996).
40. D.S. Ucker et al., Genome digestion is a dispensable consequence of physiological cell-death mediated by cytotoxic T-lymphocytes, *Mol. Cell. Biol.* **12**, 3060-3069 (1992).
41. C.E. Scott and F. Adebodun, ^{13}C-NMR investigation of protein synthesis during apoptosis in human leukemic cell lines, *J. Cell Physiol.* **181**, 147-152 (1999).
42. M.E. Moseley et al., Diffusion-weighted MR imaging of anisotropic water diffusion in cat central nervous system, *Radiology* **176**, 439-445 (1990).
43. J.M. Hakumäki et al., Quantitative ^{1}H nuclear magnetic resonance diffusion spectroscopy of BT4C rat glioma during thymidine kinase-mediated gene therapy in vivo: identification of apoptotic response. *Cancer Res.* **58**, 3791-3799 (1998).
44. S. Hortelano et al., Intracellular water motion decreases in apoptotic macrophages after caspase activation. *Cell Death Differ.* **8**, 1022-1028 (2001).
45. J.M. Hakumäki et al., Early gene therapy-induced apoptotic response in BT4C gliomas by magnetic resonance relaxation contrast T1 in the rotating frame, *Cancer Gene Ther.* **9**, 338-345 (2002).
46. O.H.J. Gröhn et al., Novel magnetic resonance imaging contrasts for monitoring response to gene therapy in rat glioma, *Cancer Res.* **63**, 7571-7574 (2003).
47. P.K. Valonen et al., Water diffusion in a rat glioma during ganciclovir-thymidine kinase gene therapy-induced programmed cell death in vivo: correlation with cell density, *J. Magn. Reson. Imaging* **19**, 389-396 (2004).
48. R. Weissleder et al., Superparamagnetic iron oxide: pharmacokinetics and toxicity, *AJR Am J Roentgenol.* **152**, 167-173 (1989).
49. R. Weissleder et al., In vivo magnetic resonance imaging of transgene expression, *Nature Med.* **6**, 351-355 (2000).
50. D. Artemov et al., Magnetic resonance molecular imaging of the HER-2/neu receptor, *Cancer Res.* **63**, 2723-2727 (2003).
51. M. Zhao et al., Non-invasive detection of apoptosis using magnetic resonance imaging and a targeted contrast agent, *Nature Med.* **7**, 1241-1244 (2001).

52. E.A. Schellenberger et al., Annexin V-CLIO: a nanoparticle for detecting apoptosis by MRI, *Mol Imaging* **1**, 102-107 (2002).
53. A. Flotats and I. Carrio, Non-invasive in vivo imaging of myocardial apoptosis and necrosis. *Eur. J. Nucl. Med. Mol. Imaging* **30**, 615-30 (2003).
54. M. Doubrovin et al., Imaging transcriptional regulation of p53-dependent genes with positron emission tomography in vivo, *Proc. Natl. Acad. Sci. USA.* **98**, 9300-9305 (2001).